J|A|C|S
ARTICLES

Published on Web 09/29/2009

Electric-Field-Induced Charge-Transfer Phase Transition: A Promising Approach Toward Electrically Switchable Devices

Tarik Mahfoud,[†,‡,§,∥] Gábor Molnár,[*,†,‡] Sébastien Bonhommeau,[†,‡] Saioa Cobo,[†,‡]
Lionel Salmon,[†,‡] Philippe Demont,[⊥] Hiroko Tokoro,[#] Shin-Ichi Ohkoshi,[#]
Kamel Boukheddaden,[∇] and Azzedine Bousseksou[*,†,‡]

CNRS, Laboratoire de Chimie de Coordination, 205 route de Narbonne, Toulouse, France, Université de Toulouse, UPS, INPT, LCC, F-31077 Toulouse, France, The Institute of Nanomaterials and Nanotechnology, iNanoTech, ENSET, Avenue de l'Armée Royale, Madinat Al Irfane, 10100 Rabat, Morocco, UFR Matériaux en couches Minces et Systèmes pour la Conversion Photovoltaïque, F. S. T. Mohammedia, Université Hassan II Mohammedia, B.P. 146, Bd Hassan II, Mohammedia, Morocco, Laboratoire de Physique des Polymères-CIRIMAT, CNRS UMR-5085 Université Toulouse III, 118 Route de Narbonne, 31062 Toulouse Cedex, France, Department of Chemistry, School of Science, The University of Tokyo, 7-3-1 Hongo, Bunkyo-ku, Tokyo 113-0033 Japan, and Groupe d'Etudes de la Matière Condensée, CNRS-Université de Versailles-St. Quentin en Yvelines, 45 Avenue des Etats-Unis, F78035 Versailles Cedex, France

Received July 13, 2009; E-mail: Gabor.Molnar@lcc-toulouse.fr; Azzedine.Bousseksou@lcc-toulouse.fr

Abstract: Much research has been directed toward the development of electrically switchable optical materials for applications in memory and display devices. Here we present experimental evidence for an electric-field-induced charge-transfer phase transition in two cyanometalate complexes: $Rb_{0.8}Mn[Fe(CN)_6]_{0.93}\cdot 1.62H_2O$ and $Co_3[W(CN)_8]_2(pyrimidine)_4\cdot 6H_2O$, involving changes in their magnetic, optical, and electronic properties as well. Application of an electric field above a threshold value and within the thermal hysteresis region leads to a transition from the high- to the low-temperature phase in these compounds. A model is proposed to explain the main observations on the basis of a para-ferroelectric transition. Our observations suggest that this new concept of electrical switching, based on materials exhibiting charge-transfer phase transitions with large thermal hysteresis loops, may open up doors for novel electro-optical devices.

Introduction

Several materials exhibit large and reversible changes in their optical properties (color, refractive index, etc.) under an externally applied electric field. Among these, the most well-known are electro-optical materials as well as electrochromic and liquid crystal systems.[1−3] However, the performance of the existing materials (cost, lifetime, energy consumption, response time, etc.) is still limited, and a great amount of research activity is currently being undertaken to improve them. On the other hand, instead of improving the existing technologies, it is important also to explore novel physical mechanisms, which may lead to electric-field-induced (EFI) switching of material properties. For example, bistable organic compounds[4] or materials exhibiting metal−insulator transitions[5] have been reported to display interesting and potentially useful switching properties under an external electrical bias.

In this context bistable coordination complexes exhibiting two close-lying electronic states represent an appealing field of investigation. Here, we focus on charge-transfer (CT) complexes, which can adopt several (meta-)stable charge-localized electronic forms differing in charge distribution.[6] Within this vast family, a few compounds display first-order thermal phase transitions associated with a metal-to-metal electron transfer.[7−12] The large thermal hysteresis loop, which accompanies in most

---

[†] CNRS, Laboratoire de Chimie de Coordination.
[‡] Université de Toulouse.
[§] iNanoTech, ENSET.
[∥] Université Hassan II Mohammedia.
[⊥] CNRS UMR-5085 Université Toulouse III.
[#] The University of Tokyo.
[∇] CNRS-Université de Versailles-St. Quentin en Yvelines.

(1) Lampert, C. M. *Sol. Energy Mater. Sol. Cells* **1998**, *52*, 207–221.
(2) Waser, R., Ed. *Nanoelectronics and Information Technology*; Wiley-VCH: 2003.
(3) Dalton, L. R.; Steier, W. H.; Robinson, B. H.; Zhang, C.; Ren, A.; Garner, S.; Chen, A. T.; Londergan, T.; Irwin, L.; Carlson, B.; Fifield, L.; Phelan, G.; Kincaid, C.; Amend, J.; Jen, A. *J. Mater. Chem.* **1999**, *9*, 1905–1920.
(4) Luo., Y.; Collier, C. P.; Jeppesen, J. O.; Nielsen, K. A.; Delonno, E.; Ho, G.; Perkins, J.; Tseng, H. R.; Yamamoto, T.; Stoddart, J. F.; Heath, J. R. *ChemPhysChem* **2002**, *3*, 519–525.
(5) Kanki, T.; Park, Y. G.; Tanaka, H.; Kawai, T. *Appl. Phys. Lett.* **2003**, *83*, 4860–4862.
(6) Kato, K.; Moritomo, Y.; Takata, M.; Sakata, M.; Umekawa, M.; Hamada, N.; Ohkoshi, S.; Tokoro, H.; Hashimoto, K. *Phys. Rev. Lett.* **2003**, *91*, 255502.
(7) Ohkoshi, S.; Tokoro, H.; Hashimoto, K. *Coord. Chem. Rev.* **2005**, *249*, 1830–1840.
(8) Ohkoshi, S.; Ikeda, S.; Hozumi, T.; Kashiwagi, T.; Hashimoto, K. *J. Am. Chem. Soc.* **2006**, *128*, 5320–5321.
(9) Ohkoshi, S.; Hamada, Y.; Matsuda, T.; Tsunobuchi, Y.; Tokoro, H. *Chem. Mater.* **2008**, *20*, 3048–3054.
(10) Sato, O.; Tao, J.; Zhang, Y. Z. *Angew. Chem., Int. Ed.* **2007**, *46*, 2152–2187; *Angew. Chem.* **2007**, *119*, 2200−2236.

10.1021/ja9055855 CCC: $40.75

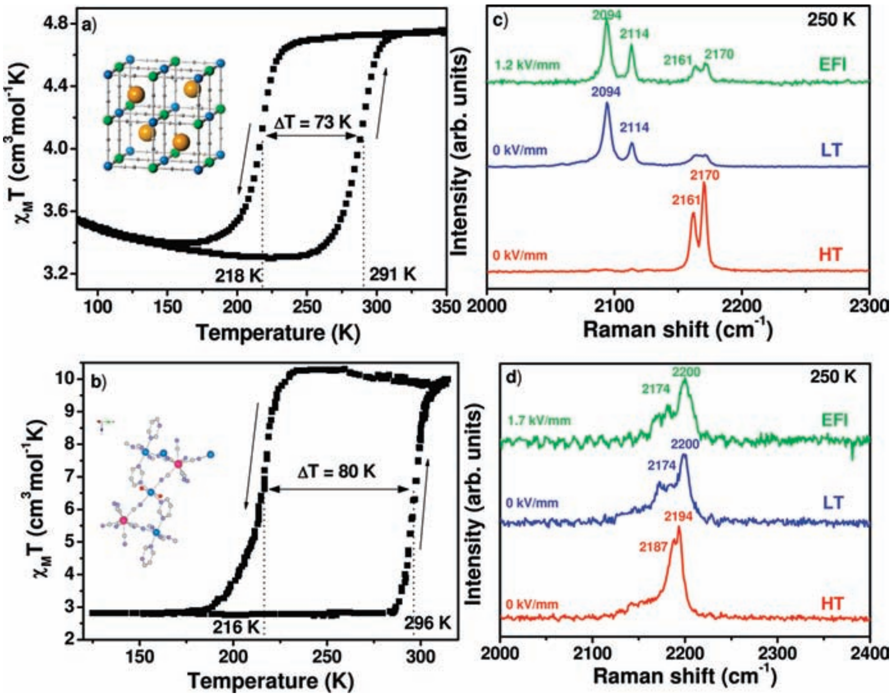

Figure 1. (Left panels) Temperature dependence of $\chi_M T$ of $Rb_{0.8}Mn[Fe(CN)_6]_{0.93}\cdot 1.62H_2O$ (a) and $Co_3[W(CN)_8]_2(pyrimidine)_4\cdot 6H_2O$ (b) in the cooling and heating modes. The inserts show the room temperature crystal structure of the corresponding compounds.[24,9] (Right panels) Raman spectra of $Rb_{0.8}Mn[Fe(CN)_6]_{0.93}\cdot 1.62H_2O$ (c) and $Co_3[W(CN)_8]_2(pyrimidine)_4\cdot 6H_2O$ (d) each recorded at 250 K in the high-temperature (HT) and low-temperature (LT) phases without any external electric field as well as under an applied field (EFI) in the ascending branch of the hysteresis.

cases these phase transitions confers a memory effect to these systems creating a fundamentally new scope for electric-field-driven switching and memory devices when the field is applied within the hysteresis region.

To test this new idea we have investigated the following three-dimensional (3D) coordination networks: $Rb_{0.8}Mn[Fe(CN)_6]_{0.93}\cdot 1.62H_2O$ (**1**) and $Co_3[W(CN)_8]_2(pyrimidine)_4\cdot 6H_2O$ (**2**). The cubic structure of the Prussian-blue type complex **1** is shown in the insert of Figure 1a. This compound exhibits a CT phase transition between the high-temperature (HT) $Fe^{III}(S = 1/2)-CN-Mn^{II}(S = 5/2)$ and the low-temperature (LT) $Fe^{II}(S = 0)-CN-Mn^{III}(S = 2)$ states, accompanied by a large thermal hysteresis loop of (mainly) elastic origin.[7] On the other hand, complex **2** is based on octacyanometalate building blocks (see insert of Figure 1b), and it was shown to display a CT phase transition between the HT $Co^{II}_{HS}(S = 3/2)-NC-W^{V}(S = 1/2)$ and the LT $Co^{III}_{LS}(S = 0)-NC-W^{IV}(S = 0)$ electronic configurations (HS and LS stand for high-spin and low-spin, respectively).[8,9] It is known from recent literature that the CT phase transition in this family of complexes can be induced by temperature, pressure or light irradiation.[7,10,11] The two phases display markedly different magnetic, optical, and electrical properties in each case, which not only can be used to follow the phase transition but also allows one to consider them for potential applications in devices. Of particular importance for optical devices is the complex dielectric permittivity ε^* exhibiting drastic variations over the visible spectrum. For example, using the ellipsometry data published in ref 12, one can estimate the refractive index and absorbance changes between the two phases at 600 nm as high as $\Delta n = 0.16$ and $\Delta k = 0.5$ in compounds analogous to **1**. In addition, the thermal hysteresis loops can be exceptionally large (up to 138 K), and they can encompass the room temperature range in certain cases.[7,9] It is also interesting to note that, in complex **2**, the CT phase transition is accompanied by a spin state conversion on the cobalt ions as well. In contrast, compound **1** does not exhibit any spin state conversion, but a cooperative Jahn−Teller distortion occurs in the LT phase on the Mn^{III} ions.

Results and Discussion

Figure 1a and b report the product of molar magnetic susceptibility and temperature for the microcrystalline samples **1** and **2** as a function of the temperature. The $\chi_M T$ value, where χ_M stands for the molar magnetic susceptibility, falls from 4.7 to 3.4 cm^3 K mol^{-1} in compound **1** and from 10.3 to 2.8 cm^3 K mol^{-1} in compound **2** on going from the HT to the LT phase. The phase transition temperatures in the cooling (heating) modes are 218 (291) and 216 (296) K for compounds **1** and **2**, yielding 73 and 80 K wide hysteresis loops, respectively. The phase transition is accompanied also by a color change from light brown (HT) to dark brown (LT) in compound **1** and from red (HT) to blue (LT) in compound **2**.

The CT phase transition can be conveniently followed in these compounds by Raman spectroscopy since they exhibit sharp and intense CN stretching modes around 2100−2200 cm^{-1}, which are known to be very sensitive to the oxidation and spin state of the coordinating metal ions.[13] Figure 1c and d show selected Raman spectra of **1** and **2** excited at 632.8 nm at 250 K in the HT and LT phases before applying an external electric

---

(11) Cartier dit Moulin, C.; Champion, G.; Cafun, J. D.; Arrio, M. A.; Bleuzen, A. *Angew. Chem., Int. Ed.* **2007**, *46*, 1287–1289; *Angew. Chem.* **2007**, *119*, 1309−1311.

(12) Loutete-Dangui, E. D.; Codjovi, E.; Tokoro, H.; Dahoo, P. R.; Ohkoshi, S.; Boukheddaden, K. *Phys. Rev. B* **2008**, *78*, 014303.

(13) Nakamoto, K. *Infrared and Raman Spectra of Inorganic and Coordination Compounds - Part B*; Wiley-Interscience: 1997.

field on the sample. In agreement with previous works[14] the HT ($Fe^{III}-CN-Mn^{II}$) phase of compound **1** reveals two CN stretching modes around 2161 and 2170 cm^{-1}, while the LT phase ($Fe^{II}-CN-Mn^{III}$) is characterized by two lower frequency modes around 2094 and 2114 cm^{-1}. On the other hand, we have found no Raman data in the literature for compound **2**, which presents two CN stretching modes in the HT as well as in the LT forms around 2187, 2194 cm^{-1} and 2174, 2200 cm^{-1}, respectively.

The most important result of the present paper is that we were able to observe clear changes in the Raman spectra of these compounds after the application of an external electric field in the HT phase within the thermal hysteresis region. As shown in Figure 1c and d these spectral changes can be unambiguously assigned to the CT phase transition between the HT and the LT forms of the compounds. It must be noted that this electric field effect was observed systematically when the transparent electrode (i.e., the surface probed by Raman spectroscopy) was negatively polarized. This electric-field-induced CT phase transition is irreversible in the sense that when the field is removed the sample does not return to the initial state. This result can be easily rationalized since the lifetime of the metastable states within the hysteresis region is virtually infinite. Furthermore, the reverse LT→HT phenomenon could not be induced in any instance by an electric field. However, the initial HT state of the samples can be restored by heating above their respective thermal transition temperatures. It should be noted that somewhat similar experiments have already been carried out on a NaCoFe-type Prussian blue analogue compound by Sato et al.,[15] but only a reversible current switching was reported by these authors, outside the hysteresis loop.

We have carried out a more detailed investigation of this phenomenon in the case of complex **1** (Figure 2), which displays significantly more intense and better resolved Raman markers for the HT and LT phases. The sample was first constrained in a stepwise manner to an increasing applied field at 280 K. Up to *ca.* 1.1 kV/mm no significant change was observed in the Raman spectra (Figure 2b) and the current flowing through the sample increased monotonically with the increasing bias. For a further slight increase of the applied field above a threshold value of *ca.* $E = 1.2$ kV/mm, the Raman modes of the LT phase appeared abruptly (Figure 2c) and the current increased also significantly (typically from ~0.1 to ~1 mA) that may be related to the fact that the LT phase is more conductive.[16] The Raman spectrum in Figure 2c was recorded immediately following the application of the field, but one should note that the spectrum acquisition takes *ca.* 2 min. We have recorded a few successive Raman spectra under a constant bias and observed that the proportion of the signal of the LT phase remains usually stable, albeit a further increase occurred in some cases with the time indicating that the conversion is relatively sluggish. Furthermore, when the field is switched off, the intensity ratio of the LT and HT modes remains constant during (at least) an hour in zero external field (Figure 2d). The application of the same field (1.2 kV/mm) but in the opposite direction (i.e., positive polarization on the transparent electrode) does not modify either the Raman spectrum (Figure 2e). Finally, when the sample is heated above the phase transition temperature to 320 K, it returns to the initial state (Figure 2f).

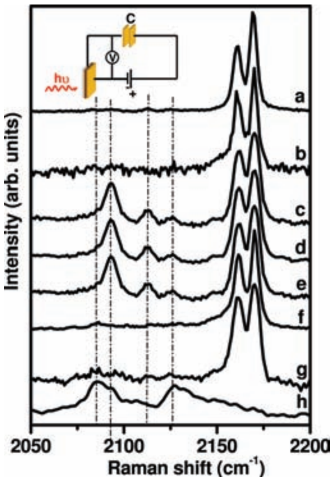

Figure 2. Electric field effect on the Raman spectra of $Rb_{0.8}Mn[Fe(CN)_6]_{0.93}\cdot1.62H_2O$. Each spectrum was acquired at 280 K successively (a) before the application of any external electric field in the HT phase, (b) after the application of a field of 1.1 kV/mm, (c) after the application of a field of 1.2 kV/mm, (d) after waiting an hour in zero external field, (e) after the application of a field of 1.2 kV/mm in the opposite direction with respect to case (c), (f) after raising the temperature to 330 K, (g) after cooling to 280 K and applying a 1.2 kV/mm field using a capacitor to block the current flow (see insert for the scheme of the circuit), and (h) after the application of a field of 3 kV/mm.

In another experiment, the sample **1** was cooled down to 280 K and was polarized by introducing a capacitor in the circuit to impede the current flow (the scheme of the circuit is shown in the insert of Figure 2). No effect could be detected up to applied fields of 3 kV/mm underlying the importance of the charge injection (Figure 2g) in the mechanism of the generated phase transition. After removing the capacitor, we have tried to apply fields higher than 1.2 kV/mm to further increase the conversion efficiency. Up to *ca.* 1.8 kV/mm, only the conversion to the LT phase occurs, but above ~1.8 kV/mm, the irreversible sample reduction starts to compete with the CT phase transition leading to the complete reduction of the sample ($Mn^{II}-NC-Fe^{II}$ form) above 2.2 kV/mm, characterized by two Raman modes around 2085 and 2128 cm^{-1} [17] (Figure 2h).

Electric field effects on Prussian blue, $KFe^{III}[Fe^{II}(CN)_6]$, exhibiting no CT phase transition, have been already studied by Carpenter et al.,[18] who observed a partial reduction of the compound near the cathode and a partial oxidation near the anode. They explained this phenomenon by the fact that Prussian blue type compounds are mixed conductors in which the alkali cations can move to provide the charge compensation required for the redox reactions. Obviously similar phenomena are expected to occur in other PB analogues as well and can thus rationalize the observed reduction in **1**. This reduction at higher fields was not observed in sample **2**.

Figure 3 displays the proportion of the HT phase before and after the application of an external electric field (~1.2 kV/mm) at different points of the hysteresis loop. For each measurement the sample was first slowly cooled down (warmed up) in the descending (ascending) branch of the hysteresis loop to the

---

(14) Cobo, S.; Fernández, R.; Salmon, L.; Molnár, G.; Bousseksou, A. *Eur. J. Inorg. Chem.* **2007**, 1549–1555.

(15) Sato, O.; Kawakami, T.; Kimura, M.; Hishiya, S.; Kubo, S.; Einaga, Y. *J. Am. Chem. Soc.* **2004**, *126*, 13176–13177.

(16) Molnár, G.; Cobo, S.; Mahfoud, T.; Vertelman, E. J. M.; van Koningsbruggen, P. J. *J. Phys. Chem. C* **2009**, *113*, 2586–2593.

(17) Bonhommeau, S.; Pontius, N.; Cobo, S.; Salmon, L.; de Groot, F. M. F.; Molnár, G.; Bousseksou, A.; Dürr, H. A.; Eberhardt, W. *Phys. Chem. Chem. Phys.* **2008**, *10*, 5882–5889.

(18) Carpenter, M. K.; Conell, R. S. *J. Electrochrom. Soc.* **1990**, *137*, 2464–2467.

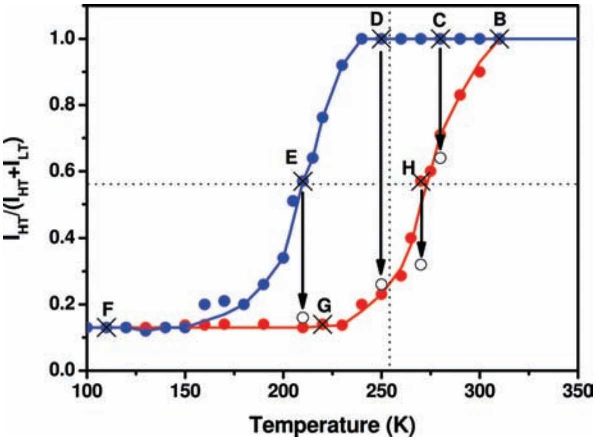

Figure 3. Electric-field-induced CT transition from different initial states. The closed circles show the temperature dependence of the Raman intensity ratio of the υ_{CN} modes of $\mathrm{Rb_{0.8}Mn[Fe(CN)_6]_{0.93}\cdot 1.62H_2O}$ in the HT and LT phases in zero applied field ($I_{HT}/(I_{HT}+I_{LT})$). The crosses (open circles) show the proportion of the HT phase before (after) the application of an electrical field of 1.2 kV/mm on different points of the hysteresis loop.

desired temperature, and it was stabilized during at least 0.5 h before the Raman spectrum of the initial state of the compound was recorded. Then, another Raman spectrum was recorded immediately after a voltage application on the sample as well as 5 min later to check the stability of the final state. The proportion of the two phases was estimated from the area ratio of the Raman υ_{CN} modes $I_{HT}/(I_{HT}+I_{LT})$. In the pure HT phase at 310 K no field effect could be observed. However, Raman spectra collected after the application of the electric field at 280 K (cooling mode) revealed a sample conversion to a state consisting of 36% LT fraction. The same experiment with fresh samples at 250 and 210 K led to a quasi-complete HT→LT phase conversion with a final state consisting of 74% and 84% LT fractions, respectively. In a similar manner, we have carried out measurements on the ascending branch as well at 110 and 220 K, but we have observed no field effect on the Raman spectra. However, at 270 K on the ascending branch of the hysteresis loop we could observe a conversion from a 43% LT initial phase to a 68% LT final phase, indicating that the hysteresis loop is modified by the electric field to some extent. This observation of the evolution of the sample properties in the electric field may be related to the nonstoichiometric, disordered nature of sample **1**. On the whole, however, it appears clearly that the electric field stabilizes the LT phase and the field-induced switch occurs within the hysteresis region. It should be noted here that we have also investigated the electric field effect on another RbMnFe analogue, which presents no CT phase transition, and observed only the apparition of the reduced form.

Conceivable mechanisms for the EFI resistive switching can involve thermal, electronic, or electrochemical phenomena. Thermal effects can be easily ruled out here since they cannot explain the HT→LT phase conversion and should facilitate the LT→HT conversion, which was not observed. Ionic transport and electrochemical redox reactions are known to occur in Prussian blue analogues under external electric fields.[18] Indeed, the appearance of the reduced form of **1** at fields above 1.8 kV/mm must originate from such a redox phenomenon. The observation of different processes occurring on the cathode and the anode as well as the fact that current flow through the sample is a necessary condition for the EFI HT→LT transition is also in line with an electrochemical phenomenon. However, if the origin of this transition is an electrochemical process one may expect it to occur not only within the hysteresis region but also outside, which is in contradiction with our observations. Another plausible cause for the HT→LT phase transition is a paraelectric−ferroelectric transition. Such a transition is known to be triggered by high electric fields and to stabilize the LT phase at the expense of the HT phase by shifting the critical temperature of the first-order thermal phase transition toward high temperatures.[19] Indeed, ferroelectricity was reported at cryogenic temperatures in RbMnFe-type compounds similar to **1**.[20] So as to further corroborate this assumption we have carried out dielectric measurements on both **1** and **2** in a wide temperature and frequency range. Figure 4 displays the temperature dependence of the real part of the complex dielectric permittivity (ε') at different frequencies. For both compounds one can note a dielectric anomaly peak in the $\varepsilon'(T)$ curves close to the phase transition temperatures, the position of which is frequency independent. This demonstrates the occurrence of a displacive, paraelectric−ferroelectric transition for compounds **1** and **2**.

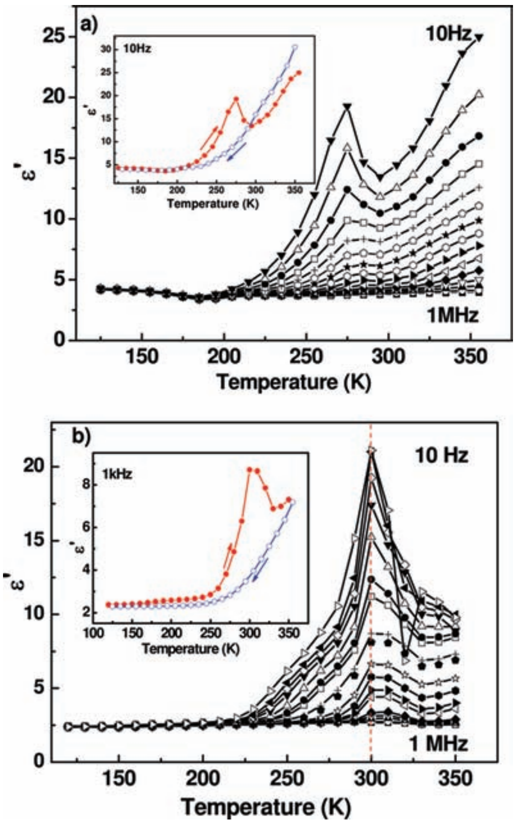

Figure 4. Temperature dependence of the real part of the complex dielectric permittivity of $\mathrm{Rb_{0.8}Mn[Fe(CN)_6]_{0.93}\cdot 1.62H_2O}$ (a) and $\mathrm{Co_3[W(CN)_8]_2(pyrimidine)_4\cdot 6H_2O}$ (b) recorded at different frequencies in the heating mode. The hysteresis curves at selected frequencies are shown in the inserts.

For compound **1**, the first-order displacive paraelectric−ferroelectric transition proceeds from the cubic ($F\bar{4}3m$) HT to the tetragonal ($I\bar{4}m2$) LT phase that is from a symmetric to a distorted phase. Considering the sample **1** as a vibronic system, which is the center of a thermally induced interplay between

---

(19) Poulsen, M.; Sorokin, A. V.; Adenwalla, S.; Ducharme, S.; Fridkin, V. M. *J. Appl. Phys.* **2008**, *103*, 034116.

(20) Ohkoshi, S.; Tokoro, H.; Matsuda, T.; Takahashi, H.; Irie, H.; Hashimoto, K. *Angew. Chem., Int. Ed.* **2007**, *46*, 3238–3241; *Angew. Chem.* **2007**, *119*, 3302−3305.

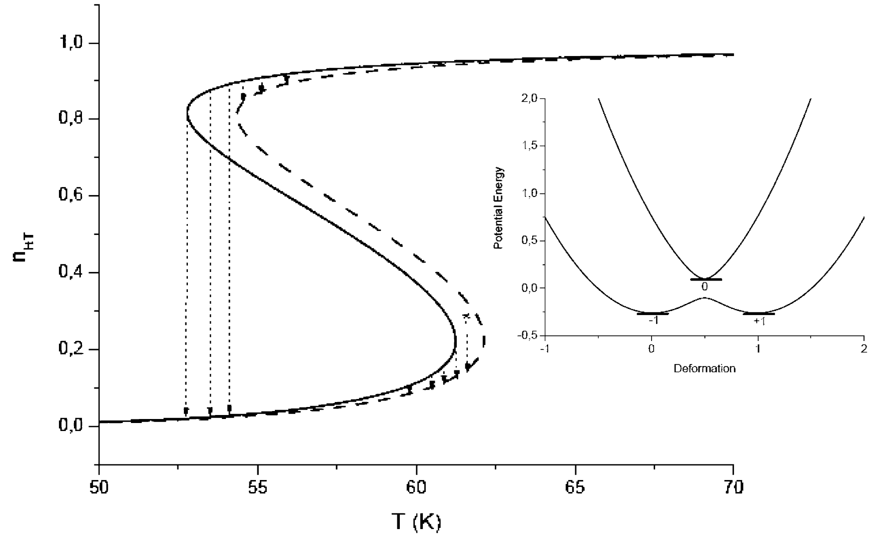

Figure 5. Effect of the electric field on the temperature dependence of the HT fraction $n_{HT}(T)$, simulated using the three-states model. The electric field stabilizes the LT (ferroelectric) phase and polarizes the dielectric system which induces a nonzero electric dipole. The arrows show the direction of the jump of the HT fraction. The insert show the configurational diagram, restricted to one effective distortion mode, showing the potential energy of the system in the LT (double well) and HT (single well) states. (See the Supporting Information for more explanations.)

ferroelectric and paraelectric phases, one can describe theoretically the potential energy of the system as formed by two types of configurational diagrams: a double well and a simple well (Figure 5), corresponding respectively to the LT and HT phases. This situation can be approximated by a three-state system by means of the well-known Blume–Capel model accounting for elastic interactions.[21] In the frame of this model, the application of a static electric field induces a shift of the transition temperature $\Delta T_{eq} = p^2E^2/\Delta H(0)$ which depends on the ratio between the square of the electrostatic energy (p is the electric dipole moment and E the external electric field) and the enthalpy change $\Delta H(0)$ at the transition (see Supporting Information for more details on the model). Considering a molecular field $E \approx 10^6$ V/m, a typical dipole moment $p \approx 2 \times 10^{-28}$ C m, and an enthalpy change $\Delta H(0) = 377$ K, it is found that the electric field shifts the whole hysteresis to higher temperatures by ~1 K, even if it causes a nonsymmetrical distortion of the thermal hysteresis loop (Figure 5). It is also evidenced that the jump of the HT fraction, resulting from the application of the electric field, takes place in one direction (from HT → LT). Moreover, its amplitude becomes maximum in the limit where the energy barrier of the metastable HT phase becomes comparable to the electrostatic energy.

For compound **2**, the same first-order displacive paraelectric–ferroelectric transition should occur from the HT phase belonging to the $P2_1/n$ centrosymmetric space group[9] to the ferroelectric LT phase whose space group is still unknown, but necessarily noncentrosymmetric to give rise to a nonzero spontaneous polarization. An order–disorder transition can be excluded in compounds **1** and **2** because of the absence of dipole moments in the unit cells of their respective HT phases and the frequency-independent peaks observed in Figure 4. The concomitant occurrence of the paraelectric–ferroelectric and magnetic transitions entails that magnetic ions (Mn and Fe in **1**, Co and W in **2**) should play an important role in the paraelectric–ferroelectric phase transition albeit vacancies,[20] alkali-metal ions,[22] and hydrogen bonding between ligand and zeolitic water molecules could also intervene.[23]

It is clear that the proposed model cannot explain all experimental findings. In particular, the absence of EFI HT → LT phase transition upon reversing the sign of the external electric field (i.e., no change observed on the anode) is difficult to explain. Furthermore, the necessity of current flow shows also that the observed phenomena are not purely field-induced. It is possible that the migration of charge carriers toward the electrodes under the field and the build-up of a space charge region facilitate somehow the switching effect, but this explanation remains purely speculative at the present stage. One should note also that in ferroelectric materials an applied electric field can also induce piezoelectricity. Taking into account the huge volume contraction when going from the HT to the LT phase (*ca.* 10% for compound **1**), such electromechanical effects may also contribute to the stabilization of the LT phase under an applied dc bias.

Conclusions

In summary, we have observed a new type of electric-field-induced transition near room temperature within the thermal hysteresis region of transition metal complexes exhibiting charge-transfer phase transition phenomena. Of central interest in this family of compounds are the facts that this transition is accompanied by a spectacular change of material properties (magnetic, optical, electrical, and mechanical) and also that the material properties can be tuned to a great extent by synthetic chemistry methods. The EFI transition takes place from the high-temperature toward the low-temperature phase, but the inverse switch can easily be achieved as well by a thermal–electrical (Joule) effect, leading to an all-electrical device. We believe

---

(21) Boukheddaden, K.; Nishino, M.; Varret, F. *Phys. Rev. B* **2005**, *72*, 014467.

(22) Bleuzen, A.; Escax, V.; Ferrier, A.; Villain, F.; Verdaguer, M.; Münsch, P.; Itié, J. P. *Angew. Chem., Int. Ed.* **2004**, *43*, 3728–3731; *Angew. Chem.* **2004**, *116*, 3814–3917.

(23) Nakagawa, K.; Tokoro, H.; Ohkoshi, S. *Inorg. Chem.* **2008**, *47*, 10810–10812.

(24) Vertelman, E. J. M.; Lummen, T. T. A.; Meetsma, A.; Bouwkamp, M. W.; Molnár, G.; van Loosdrecht, P. H. M.; van Koningsbruggen, P. J. *Chem. Mater.* **2008**, *20*, 1236–1238.

that the mechanism of this phenomenon is related to a paraelectric−ferro(piezo)electric transition through the field-induced stabilization of the low-temperature phase, but further investigations on the mechanism of this phase transition will be necessary using microscopic and structural probes such as X-ray diffraction under high electric fields. From the theoretical point of view, this effect can be well described using simple qualitative models, which capture the essential features of the phenomenon.

Experimental Section

Sample Synthesis and Characterization. The microcrystalline powder of $Rb_{0.8}Mn[Fe(CN)_6]_{0.93}\cdot 1.62H_2O$ (**1**) was prepared by slowly adding an aqueous solution (50 mL) of $MnCl_2\cdot 4H_2O$ (2.5 mmol) to an aqueous solution (50 mL) of $K_3[Fe(CN)_6]$ (2.5 mmol) and RbCl (25 mmol). The solution was stirred mechanically and kept at a temperature of 50 °C during the addition procedure and over a successive hour. The brown powder precipitate was filtered, washed with Millipore H_2O, and dried in air at room temperature. Elemental analysis calculated for $Rb_{0.8}Mn[Fe(CN)_6]_{0.93}\cdot 1.62H_2O$ (358.10 g/mol): calcd. Rb 19.12, M_n 15.55, Fe 14.69, C 18.95, N 22.11; found Rb 19.12, M_n 15.55, Fe 14.13, C 19.70, N 23.11, H_2O 8.18. All chemicals were purchased from Sigma-Aldrich and used without purification. The powder of $Co_3[W(CN)_8]_2(pyrimidine)_4\cdot 6H_2O$ (**2**) has been synthesized as described in ref 9. The charge-transfer phase transition was confirmed in each sample by magnetic susceptibility measurements, which were carried out by means of a Quantum Design MPMS magnetometer at heating and cooling rates of 1 K min^{-1}. The experimental data were corrected for the diamagnetic contribution.

Raman Spectroscopy under Electrical Bias. The fine powder samples (*ca.* 3 mg with an effective diameter of 3 mm) were pressed between two electrodes, a metallic one and an ITO (indium−tin oxide) deposited on a transparent glass plate. This "cell" was attached to the coldfinger of an Optistat-CF Oxford Instruments He exchange gas cryostat. Raman spectra were collected between 320 and 80 K using a LabRAM-HR (Jobin-Yvon) Raman spectrometer (600 grooves/mm grating, 100 μm entrance slit, ~3 cm^{-1} spectral resolution) coupled to a CCD detector (Andor DU420) and an Olympus BXFM optical microscope. Raman scattering was excited at 632.8 nm by means of a HeNe laser with 0.07 mW excitation power on the sample. The laser beam was focused on the sample via a long-working-distance X50 microscope objective, which served also to collect the scattered photons. The Rayleigh scattering was removed by a holographic notch filter, and the Raman spectra were recorded between 1800 and 2400 cm^{-1} with typical acquisition times of 2−5 min. We used a Keithley model 6430 source-meter to apply voltages up to 210 V on our sample and to control its resistivity during the experiments. Field values indicated in the body text are deduced from voltages applied according to the source-meter and not the genuine values at the sample because losses, due to the geometry of the electrodes and to the sample heterogeneity notably, could not be assessed reliably. In most cases, at the interface with the ITO electrode (cathode) the powder sample was not homogenously converted by the electric excitation probably due to an imperfect contact with the electrode.

Dielectric Measurements. Dielectric measurements were carried out on powder samples enclosed between two metallic electrodes using a Novocontrol BDS 4000 broadband dielectric spectrometer coupled to a Quatro Cryosystem. Frequency sweeps (10^{-2}−10^{6} Hz) were carried out isothermally in the 120−350 K temperature range.

Acknowledgment. We are grateful to L. Rechignat (LCC-CNRS) for technical assistance. Financial support from the EU NoE MAGMANET project and the LIA-229 (French-Moroccan Associated Laboratory) is acknowledged.

Supporting Information Available: Theoretical model accounting for the electric-field-induced CT phase transition. This material is available free of charge via the Internet at http://pubs.acs.org.

JA9055855